

## Structural, Optical And Surface Morphological Properties of Nanosized Nickel Ferrite Particles By Co-Precipitation Method

R. Asokarajan<sup>1</sup>, A. Milton Franklin Benial<sup>2</sup>  
and K. Neyvasagam<sup>3\*</sup>

<sup>1</sup>*Department of Physics, VHNSN College, Virudhunagar – 626 001, India.*

E-mail: rasokarajan@gmail.com

<sup>2</sup>*Department of Physics, NMSSVN College, Madurai – 625 019, India.*

E-mail: miltonfranklin@yahoo..com

<sup>3\*</sup>*Department of Physics, The Madura College, Madura - 625 011, India.*

E-mail: srineyvas@yahoo.co.in

### Abstract

Nanocrystalline inverse spinel structure of nickel ferrite (NiFe<sub>2</sub>O<sub>4</sub>) has been synthesized by the co-precipitation method in an aqueous medium. The crystallinity, grain size and microstructure of the synthesized nanoparticles were performed by X-ray powder diffraction (XRD) and Scanning Electron Microscopy(SEM). Optical UV–Visible absorption and FTIR spectrum have been performed to examine the band gap and chemical compositions of NiFe<sub>2</sub>O<sub>4</sub> nanoparticles. The characteristic peaks match well with the reported values and no secondary phase was detected in XRD, ensuring the phase purity of the final product. Based on the Scherrer's formula, an average crystalline size was 35nm. SEM image shows the particles as homogeneous in nature. Fourier transform infrared spectroscopy(FTIR) confirmed the presence of metal oxide band. The band gap of the nanocrystalline NiFe<sub>2</sub>O<sub>4</sub> was 3.98eV determined by UV-Visible spectrum.

**Keywords:** Nickel Ferrite, Nanoparticle, XRD, SEM, UV-Visible and FTIR.

## 1. Introduction

Nanosized spinel ferrites of the  $\text{NiFe}_2\text{O}_4$  have been greatly increased in the past few years due to their importance in understanding the fundamentals in nanoscale magnetism and their wide range of applications such as high-density data storage, microwave devices, ferro-fluid technology, sensor technology, spintronics, magnetocaloric refrigeration, heterogeneous catalysis, magnetically guided drug delivery and magnetic resonance imaging [1,2]. Also, their applications include fabrication of magnetic cores of read or write heads for high-speed digital tape or disk recording [3]. Bulk  $\text{NiFe}_2\text{O}_4$  is a soft ferrimagnetic material with completely inverse spinel structure [4]. Also, the nanoparticle of  $\text{NiFe}_2\text{O}_4$  exhibits unusual physical and chemical properties when its size is reduced into the nano-region. Nickel ferrite has been studied extensively due to their different structures composed of inverse, normal, and mixed spinel structures respectively, and their high electromagnetic performance, excellent chemical stability, mechanical hardness, low coercivity, and moderate saturation magnetization make it a good contender for the application as soft magnets and low-loss materials at high frequencies [5–7]. These properties are dependent on the chemical composition and microstructural characteristics in which the particle size and shape might be controlled in the fabrication processes. For this wide variety of usage, nanocrystalline  $\text{NiFe}_2\text{O}_4$  has been studied by many investigators [8] and these Nanosized materials are also prepared in the forms of thin film, powder and colloid using different synthesis techniques such as wet chemical routes, sol-gel, sputtering, co-evaporation, hydrothermal synthesis, high energy ball milling, chemical co-precipitation, micro-wave irradiation and ultrasonic irradiation method [9, 10]. In this paper, nanocrystalline nickel ferrite,  $\text{NiFe}_2\text{O}_4$ , was synthesized by co-precipitation method. The synthesized nanoparticle was characterized by powder X-ray powder diffraction (XRD), Scanning Electron Microscopy (SEM), UV-Visible spectra and Fourier Transform Infrared Spectroscopy (FTIR).

## 2. Experimental Details

### 2.1 Synthesis of $\text{NiFe}_2\text{O}_4$ nanoparticles

All chemicals and solvents were obtained from AR grade and used without further purification. Nickel ferrite ( $\text{NiFe}_2\text{O}_4$ ) nanopowders were synthesized by co-precipitated methods, from nitrate precursors. Stoichiometric amount of  $\text{Ni}(\text{NO}_3)_2 \cdot 6\text{H}_2\text{O}$  and  $\text{Fe}(\text{NO}_3)_3 \cdot 9\text{H}_2\text{O}$  were dissolved in aqueous ethanol solution and mixed to the precipitation agent with aqueous  $\text{NH}_4\text{OH}$  solution and the solution was stirred for 6 hours under a high stirring rate condition using magnetic stirrer at room temperature.



The final solution was collected and filtered. The synthesized  $\text{NiFe}_2\text{O}_4$  was filtered off, washed with distilled water, then used absolute ethanol with acetone to remove the free water content from the particle surface and dried in an oven at 90 – 95° C. Finally  $\text{NiFe}_2\text{O}_4$  nano powder was obtained.

## 2.2. Characterization

Powder X-ray diffraction (XRD) patterns were recorded with a Bruker AXS D8 Advance powder X-ray diffractometer (X-ray source: Cu, Wavelength 1.5406 Å). The X-ray diffraction (XRD) results were compared using the Joint Committee Powder Diffraction Standards (JCPDS) data for the phase identification (See Table-1). The morphology was determined by scanning electron microscopy using Hitachi SEM S2460N model (SEM). FTIR spectra are recorded using KBr pellets on a Shimadzu 8400S FT-IR spectrophotometer, in the range of 4000 - 400 cm<sup>-1</sup>. The synthesized NiFe<sub>2</sub>O<sub>4</sub> nanoparticles optical absorption spectra are recorded in aqueous ethanol solution with a Perkin Elmer Lambda-20 UV/Visible spectrophotometer in the range of 200 - 1200 nm .

## 3. Results and Discussion

### 3.1. XRD Studies:

Powder X-ray diffraction studies are useful to determine the structure and particle size of the synthesized nanoparticles and also used to obtain further evidence about the structure of the nanoparticles. The observed *d*-space values of the NiFe<sub>2</sub>O<sub>4</sub> nanoparticles are compared with the standard *d*-space values of the free Nickel(II) and NiFe<sub>2</sub>O<sub>4</sub> nanoparticles from JCPDS data file. The experimental *d*-space values of the NiFe<sub>2</sub>O<sub>4</sub> nanoparticles match with the JCPDS data *d*-space values ( See Table 1 ).

**Table 1.** Powder X-ray diffraction pattern of NiFe<sub>2</sub>O<sub>4</sub> nanoparticle

Experimental <i>d</i> -space value [Å]	Standard <i>d</i> -space value [Å]	
NiFe <sub>2</sub> O <sub>4</sub>	Ni (89-7129)	NiFe <sub>2</sub> O <sub>4</sub> (10-0325)
4.981	2.271	4.820
2.952	2.161	2.948
2.563	2.010	2.513
2.456	1.565	2.408
1.964	1.311	1.913
1.610	1.216	1.703
1.423	1.135	1.605
1.230	1.121	1.476
1.146	1.098	1.410
1.132		1.271
1.096		1.203
0.962		1.086
		0.956
		0.932

From this table, the  $d$ -space value (JCPDS data file) of the free Nickel(II) and their  $\text{NiFe}_2\text{O}_4$  nanoparticles are well agreed with the experimental  $d$ -space values of the  $\text{NiFe}_2\text{O}_4$  nanoparticles, which is confirmed the presence of metal atom and  $\text{NiFe}_2\text{O}_4$  nanoparticles. The X-Ray diffraction study reveals that this powder has the well known spinel cubic structure.

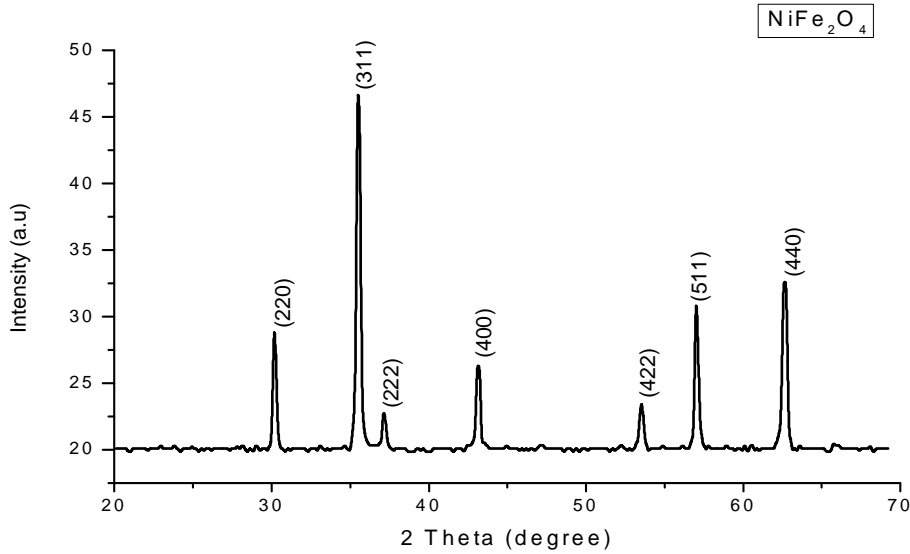


**Figure 1** XRD pattern of  $\text{NiFe}_2\text{O}_4$  Nanoparticle

From XRD patterns it was noted that there are broadening in peaks which are good indication to forming the crystalline in nano-size and size of the  $\text{NiFe}_2\text{O}_4$  was 37nm. The X-ray lines show considerable broadening, indicating the fine particle nature of the ferrite. The observed peaks at (220), (311), (222), (400), (422), (511), and (440) confirmed the spinel structure of the samples. No extra peak other than  $\text{NiFe}_2\text{O}_4$  has been found. The grain size of the crystallite (diameter  $D$ ) was determined from the full width at half maximum ( $\beta$ ) of the (220), (311), (511) and (440) peaks by using Debye – Scherer’s equation [11, 12] as

$$D = 0.9 \lambda / \beta \cos \theta \quad (1)$$

where  $\lambda$  is the wavelength of the X-ray radiation ( $\lambda = 1.5406 \text{ \AA}$ ),  $\beta$  is the full width half maximum of the characteristic peak (in radians) corrected for instrumental broadening,  $\theta$  is Bragg diffraction angle for the  $hkl$  plane and  $D$  is the grain size (nm). The calculated size is found between 35nm.

### 3.2 SEM studies

SEM allows imaging of individual crystallites and the development of a statistical description of the size and shape of the particles in a sample. The overall morphology of the particle show uniform thickness with smooth interface having perfect regular shape is given in Figure 3.

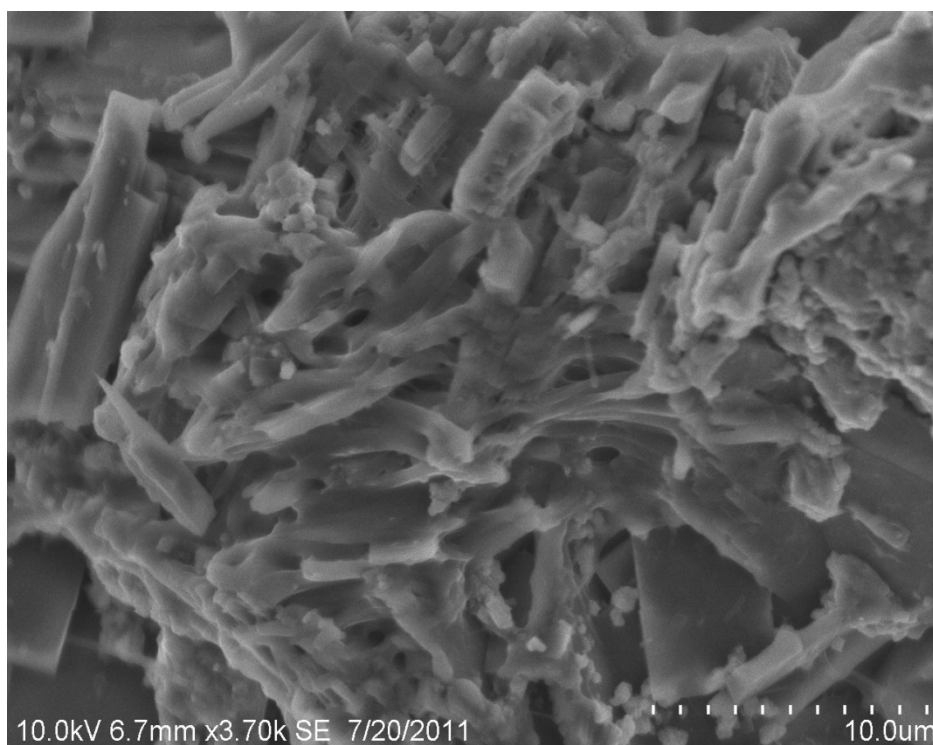


**Figure 3** SEM image of NiFe<sub>2</sub>O<sub>4</sub> Nanoparticle

A broad size distribution is observed. It consists of nearly octahedral crystals with an average size of about 40 nm. However, an actual particle size calculated through X-ray diffraction is below 40 nm.

### **3.3. Optical absorption spectral studies**

Optical properties of the synthesized NiFe<sub>2</sub>O<sub>4</sub> nanoparticle were determined from electronic absorption measurement in the range 200 - 800 nm. The optical absorption spectra of the NiFe<sub>2</sub>O<sub>4</sub> show the absorption peak around 325 nm. The absorption onset wavelength of bulk NiFe<sub>2</sub>O<sub>4</sub> is at 385 nm. This confirms the blue shift in the band gap of the synthesized sample in comparison to that of bulk NiFe<sub>2</sub>O<sub>4</sub> due to the quantum confinement effect. The energy band gap of these materials was determined by the optical absorption spectra. According to the Tauc relation, the absorption coefficient,  $a$ , for direct band gap material is given by [13]

$$Ah\nu = A(h\nu - E_g)^n \quad (2)$$

where  $E_g$  the energy gap, constant  $A$  is different for different transitions,  $(h\nu)$  is energy of photon and  $n$  is an index which assumes the values 1/2, 3/2, 2 and 3 depending on the nature of the electronic transition responsible for the reflection.

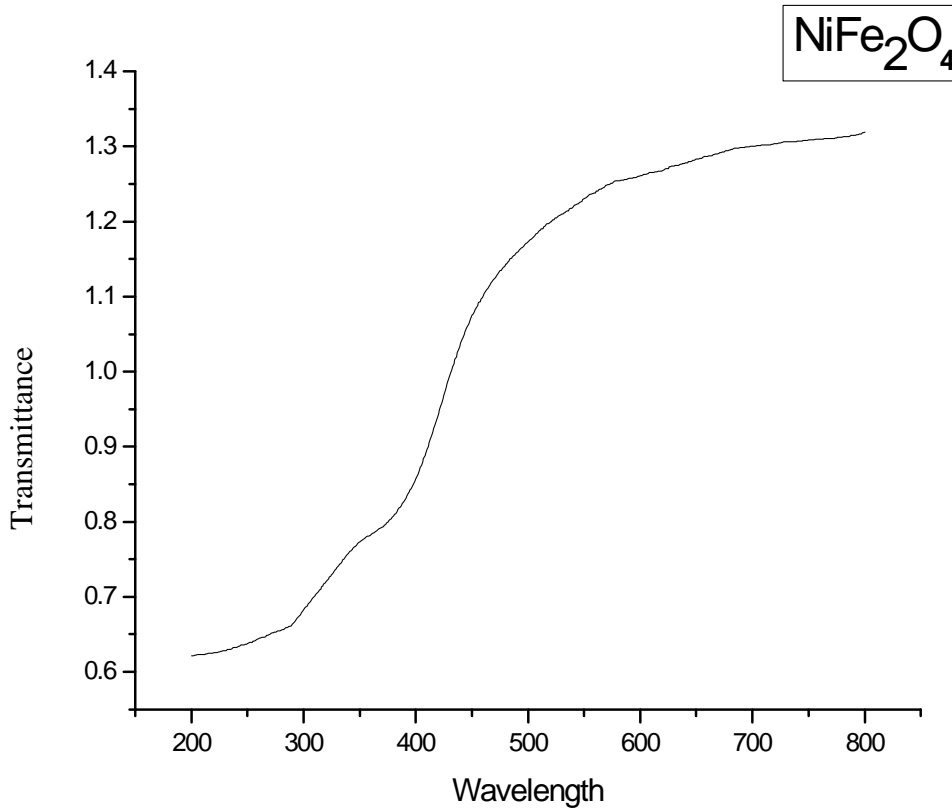


**Figure 3** UV-Visible image of NiFe<sub>2</sub>O<sub>4</sub> nanoparticle

Direct band gap ( $E_g$ ) of the sample is evaluated by plotting  $(\alpha hv)^2$  against  $hv$  and then extrapolating the straight portion of the curve on  $hv$  axis. The calculated band gap value are 3.98 eV for NiFe<sub>2</sub>O<sub>4</sub> nanoparticle, this value is higher than the bulk value (3.60 eV) of NiFe<sub>2</sub>O<sub>4</sub>. Particle size has been calculated by putting the band gap value in Brus equation [14] and it was found to be 34.6 nm.

### 3.4. FTIR studies

The IR spectra provide valuable information regarding the nature of the functional group attached to the metal ion. Figure 4 shows the FTIR absorption spectra of nanocrystalline NiFe<sub>2</sub>O<sub>4</sub> samples. They were recorded in the range of 400-4000 cm<sup>-1</sup>. From the Figure 4, the two main metal-oxygen bands at 605 and 450 cm<sup>-1</sup> are observed in the FT-IR spectrum of the synthesized NiFe<sub>2</sub>O<sub>4</sub> sample. In all spinel and particularly in ferrites, two main broad metal oxygen bands are seen in the FTIR spectra. These two bands are usually assigned to vibration of ions in the crystal lattices [15]. This is indicating the presence of uniformly distributed ferrite particles.

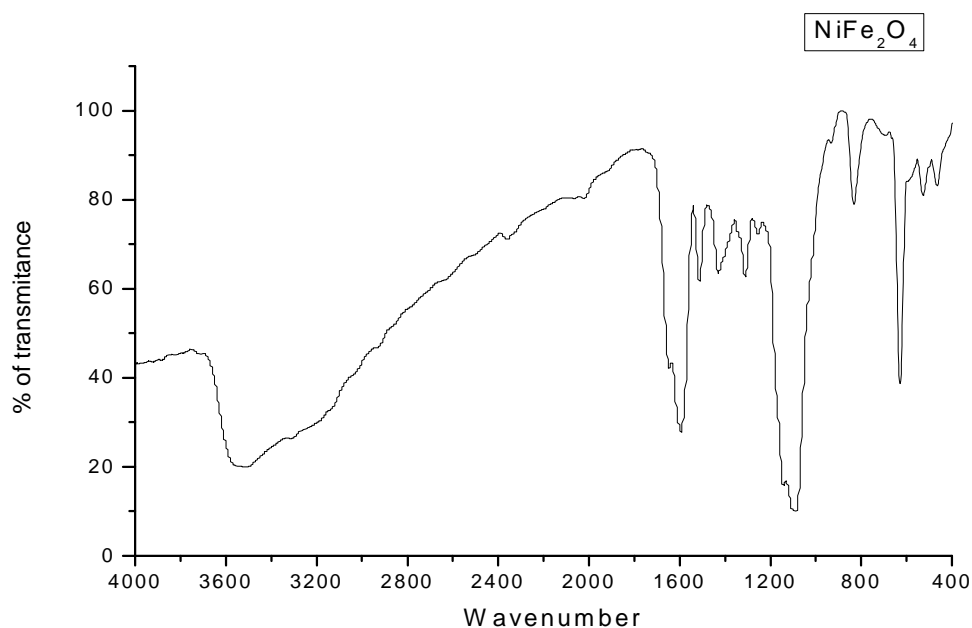


**Figure 4** FTIR spectra of NiFe<sub>2</sub>O<sub>4</sub> nanoparticle

#### 4. Conclusion

NiFe<sub>2</sub>O<sub>4</sub> binary nanoparticle powder has been synthesized by Co-precipitation method. X-ray diffraction study shows the formation of NiFe<sub>2</sub>O<sub>4</sub> nanoparticle as size of 35nm with the preferential orientation along [311]. The structure of NiFe<sub>2</sub>O<sub>4</sub> has been octahedral morphology. The FTIR spectrum of the NiFe<sub>2</sub>O<sub>4</sub> ferrite sample is given a clear indication of two vibrational bands of metal oxygen. The UV-Visible measurement shows that the band gap energy of the synthesized NiFe<sub>2</sub>O<sub>4</sub> nanoparticle was 3.98eV. From the results, these NiFe<sub>2</sub>O<sub>4</sub> nanoparticles are very good material for electronic devices technology and bionanoscience applications.

#### References

- [1] Kodama, R.H.,1999,J. Magn. Magn. Mater.,200, 359.
- [2] Prasad, S., and Gajbhiye, N. S., 1998,J. Alloys Compd.,265, 87.
- [3] Igarashi. H.,Okozaki. K., 1977, J. Am. Ceram. Soc.,60,51.
- [4] Kurikka, V.,Shafi, P.M,Koltypin, Y. and Gedanken, A., 1997,J. Phys. Chem B., **101**, 6409.
- [5] Maggioni, G., Vomiero, A.,Carturan, S., et al., 2004,“Structure and optical properties of Au-polyimide nanocomposite films prepared by ion implantation,” *Applied Physics Letters*, vol. 85, no. 23, pp. 5712–5714.
- [6] Bogle, K.A., Dhole, S.D., and Bhoraskar, V.N., 2006,“Silver nanoparticles: synthesis and size control by electron irradiation,” *Nanotechnology*, vol. 17, no. 13, pp. 3204–3208.

- [7] P. Gangopadhyay, R. Kesavmoorthy, S. Bera et al., 2005, "Preferential facet of nanocrystalline silver embedded in polyethylene oxide nanocomposite and its antibiotic behaviors," *Physical Review Letters*, vol. 94, pp. 47403–47404.
- [8] Kodama, T., Wada, Y., Yamamoto, T., Tsuji, M., Tamamura, Y., 1995, *J. Mater. Chem.*, 5(9) 1413.
- [9] Pannaprayil, T., Marande, R., Komarneni, S., Sankar, S.G., 1988 *J. Appl. Phys.*, 64, 5641.
- [10] Ceylan, S. Ozcan, C. Ni, Shah, S.I., 2008, *J. Magn. Magn. Mater.*, 320, 857.
- [11] Estermann, M.A., David, W.I.F., 2002, *Structure determination from powder diffraction data (SDPD)*, Oxford Science Publications, New York.
- [12] Guinier, A., 1963, *X-Ray diffraction*, Freeman, San Francisco, CA, USA.
- [13] Sirohi, S., and Sharma, T.P., 1999, *Opt. Mater.*, 13, 267.
- [14] Brus, L., 1991, *Appl. Phys. A: Solid Surf.*, 53, 465.
- [15] Nakamoto, K., 1986, *Infrared and Raman Spectra of Inorganic and Coordination compounds*, Wiley, New York.